PCCP

PAPER

View Article Online
View Journal | View Issue

Cite this: *Phys. Chem. Chem. Phys.*, 2016, **18**, 5324

Concentration dependent effects of urea binding to poly(*N*-isopropylacrylamide) brushes: a combined experimental and numerical study†

Samantha Micciulla,[a] Julian Michalowsky,[b] Martin A. Schroer,[cd] Christian Holm,[b] Regine von Klitzing[a] and Jens Smiatek*[b]

The binding effects of osmolytes on the conformational behavior of grafted polymers are studied in this work. In particular, we focus on the interactions between urea and poly(*N*-isopropylacrylamide) (PNIPAM) brushes by monitoring the ellipsometric brush thickness for varying urea concentrations over a broad temperature range. The interpretation of the obtained data is supported by atomistic molecular dynamics simulations, which provide detailed insights into the experimentally observed concentration-dependent effects on PNIPAM–urea interaction. In particular, in the low concentration regime ($c_u \leq 0.5$ mol L^{-1}) a preferential exclusion of urea from PNIPAM chains is observed, while in the high concentration regime ($2 \leq c_u \leq 7$ mol L^{-1}) a preferential binding of the osmolyte to the polymer surface is found. In both regimes, the volume phase transition temperature (T_{tr}) decreases with increasing urea concentration. This phenomenon derives from two different effects depending on urea concentration: (i) for $c_u \leq 0.5$ mol L^{-1}, the decrease of T_{tr} is explained by a decrease of the chemical potential of bulk water in the surrounding aqueous phase; (ii) for $c_u \geq 2$ mol L^{-1}, the lower T_{tr} is explained by the favorable replacement of water molecules by urea, which can be regarded as a cross-linker between adjacent PNIPAM chains. Significant effects of the concentration-dependent urea binding on the brush conformation are noticed: at $c_u = 0.5$ mol L^{-1}, although urea is loosely embedded between the hydrated polymer chains, it enhances the brush swelling by excluded volume effects. Beyond 0.5 mol L^{-1}, the stronger interaction between PNIPAM and urea reduces the chain hydration, which in combination with cross-linking of monomer units induces the shrinkage of the polymer brush.

Received 7th December 2015,
Accepted 21st January 2016

DOI: 10.1039/c5cp07544k

www.rsc.org/pccp

1 Introduction

Osmolytes are low-weight organic molecules which contribute to the regulation of the osmotic pressure inside the cells. Their presence allows biological cells to counteract a change of the external osmotic pressure in such a way that the isotonic balance is ensured. In addition, osmolytes have a strong influence on the structural conformation of proteins.[1–4] It was reported that in high concentrated solutions of denaturants like guanidinium chloride or urea, protein unfolding occurs when a critical osmolyte concentration is reached.[5–9] In contrast, the stabilization of protein structures was validated for protectants like trimethylamine-*N*-oxide (TMAO) and hydroxyectoine.[10–13]

Experimental findings further evidenced that low concentrations of urea and guanidinium chloride can even stabilize protein native structures[9] and lead to the fluidization of lipid bilayers and monolayers.[12–14] The mechanisms and the different accumulation properties[15–18] for protectants and denaturants around molecular surfaces can be brought into relation with the 'law of matching water affinities'.[15,19,20] As it was also recently demonstrated by computer simulations, the resulting binding behavior is a consequence of a subtle interplay between enthalpic and entropic effects, and the underlying charge of the solvated surface.[21] In addition, further simulations of thermoresponsive polymers in presence of different salt concentration also reveal a concentration dependent change of binding properties for chaotropic salts.[22] The possibility of investigating these effects is reasoned by the fact that the binding or the exclusion mechanism of the co-solute has a crucial influence on the stability of the macromolecule and therefore on the corresponding transition temperatures. Two distinct osmolyte binding mechanisms have been proposed: (1) direct interactions, related to the binding of the osmolyte to the surface of the macromolecule *via* hydrogen

[a] *Stranski-Laboratorium, Institut für Chemie, Technische Universität Berlin, D-10623 Berlin, Germany*
[b] *Institut für Computerphysik, Universität Stuttgart, D-70569 Stuttgart, Germany. E-mail: smiatek@icp.uni-stuttgart.de*
[c] *Deutsches Elektronen-Synchrotron DESY, D-22607 Hamburg, Germany*
[d] *The Hamburg Centre for Ultrafast Imaging (CUI), D-22761 Hamburg, Germany*
† Electronic supplementary information (ESI) available. See DOI: 10.1039/c5cp07544k

bonds, salt bridges or dispersion interactions,[23–27] and (2) indirect interactions, mostly imposed by the influence of the osmolyte on the local water shell around the surface.[28,29] However, it is still under debate which mechanism is predominant.

Due to the chemical variety and structural complexity, simplified homopolymers are more preferred than proteins in fundamental studies. Among them, poly(*N*-isopropylacrylamide) (PNIPAM) received a lot of scientific attention, because the mechanism underlying its thermoresponsive behavior, namely a coil-to-globule transition above the lower critical solution temperature (LCST), is closely related to the loss of protein structure upon addition of denaturating agents and resembles the behavior found for the cold denaturation of proteins.[30] It has been validated that the predominant effects displayed above the LCST rely on the low number of hydrating water molecules bound to the macromolecule.[31–35] Hence, the analysis of hydration properties, molecular size and transition temperatures represents a valid tool to study the influence of added solutes on the temperature-induced conformational changes of PNIPAM.[36,37]

In particular for PNIPAM, recent studies found that highly concentrated urea solutions lead to a significant decrease of the LCST.[38] From the results of Fourier transformed infrared spectroscopy experiments, it was concluded that mainly direct interactions between urea and the carbonyl group of NIPAM promote the collapse into a globular state *via* a stabilizing bivalent hydrogen bond. In addition, more recent numerical studies also indicated that entropic effects arising from the accumulation of urea clouds around the PNIPAM molecule might have a crucial influence on the thermal behavior.[27,39,40]

Typical studies of PNIPAM–urea interactions were performed in bulk[41–44] and very rarely for osmolyte concentrations as low as 0.5 mol L^{-1}. Indeed, grafted chains are the base of a large number of smart coatings,[45–47] therefore their conformational behavior in presence of osmolytes is of high interest. In this work, for the first time a systematic investigation of the swelling and collapse properties of PNIPAM brushes over a broad range of urea concentration from 0.1 to 7 mol L^{-1} is presented. The experimental approach consisted in monitoring the optical thickness of PNIPAM brushes by ellipsometry as a function of temperature for urea concentrations between 0.1 and 7 mol L^{-1}. From the obtained data, the transition temperature (T_{tr}) and the swelling degree (ϕ_{sw}) of PNIPAM below (288 K) and above (328 K) the critical solution temperature were calculated. The hydration properties with regard to the underlying polymer–urea interactions were deduced from the observed swelling and collapse behavior. The interpretation of the experimental data is validated by atomistic MD simulation of PNIPAM chains in two different concentration regimes (low and high molar concentration) and for temperatures below and above the phase transition. The numerical studies further allow us to elucidate the balance between solvent (water) and co-solute (urea) binding on the conformational equilibrium of the polymer chain for the different combinations of urea concentration and temperature. In particular, at low molar urea concentrations, the observed shift of the transition temperature was governed by the dilution effect of urea on bulk water, which changes its chemical potential from pure solvent to dilute solution, and therefore favors brush dehydration across the phase transition. This effect was due to a preferential exclusion of urea from the macromolecule. In contrast, at high molar urea concentrations, the preferential binding of urea to PNIPAM was responsible for the pronounced decrease of T_{tr}, which was reasoned by the weakening of PNIPAM–water interactions, and the cross-linking of the osmolyte between adjacent PNIPAM chains.

Our study offers a deeper understanding on the impact of direct urea binding and indirect effects on the conformational equilibrium of the polymer. It contributes to widen the previous knowledge in this field and to understand the behavior of proteins in presence of osmolytes.

2 Experimental section

2.1 Materials

Silicon wafers (Siltronic AG, Germany) were used as solid substrates for the polymer brushes. *N*-Isopropylacrylamide (NIPAM) (98%, stabilized by methylhydroquinone) was purchased from TCI Tokyo Chemical Industry; *N*,*N*,*N*′,*N*″,*N*″-pentamethyldiethylene-triamine (PMDETA), Cu(I)Cl, methanol and urea were all purchased from Sigma Aldrich (Germany). All reagents were used as received without any further purification.

2.2 Synthesis of polymer brushes

Polymer brushes were grown from silicon wafers by Atom Transfer Radical Polymerization (ATRP).[48] First of all, a self-assembled monolayer of the ATRP initiator 2-bromo-2-methyl-*N*-[3-(triethoxysilyl)-propyl]-propanamide (BTPAm)[49] in dry toluene (4 μL/10 mL) was adsorbed on the substrates for 24 h. A polymerization mixture of 2.83 g NIPAM in 50 mL of methanol and water (1 : 1 v/v), 183 μL *N*,*N*,*N*′,*N*″,*N*″-pentamethyldiethylene-triamine (PMDETA) and 25 mg copper(I) chloride was prepared and degassed by N_2 bubbling for 40 minutes. The initiator-modified substrates were soaked in the reaction mixture and the polymerization was run for 8 minutes, followed by termination in water/methanol mixture and thorough rinsing in Milli-Q water. The grafting density σ was calculated considering the molecular structure of the initiator and the measured thickness of the self-assembled monolayer (details are reported in the ESI†). A value of $\sigma \sim 0.4$ nm^{-2} was estimated, which corresponds to a moderate brush regime[50] and allows urea to access the full solvent accessible surface area of PNIPAM. The brush thickness of the dry state (1.9 ± 0.1% r.h.) was measured by ellipsometry after drying the samples in a sealed cell flushed with nitrogen stream for 20 minutes. The measured value was d_{dry} = (40.5 ± 0.9) nm and it remained constant for at least 10 minutes.

The molecular weight (M_W) of PNIPAM chains was estimated from the grafting density σ and the dry thickness d_{dry}, according to the relation[49,51,52]

$$M_W = \frac{\rho d_{dry} N_A}{\sigma} \quad (1)$$

with ρ the polymer mass density (1.1 g mL^{-1}) and N_A the Avogadro number. The obtained value for M_W was $\approx$67 000 g mol^{-1} (*ca.* 590 monomers per chain). Reported polydispersity indices (PDI) for ATRP polymerization are mostly between 1.2 and 1.5.[53,54] A low PDI is also expected for our system, given the low standard deviation of the brush thickness (*ca.* 0.8% of the brush thickness). The swollen thicknesses of PNIPAM brushes in solutions of urea at different concentrations varied between 100 and 150 nm at 288 K, and between 47 and 80 nm at 328 K. The values are reported in Table S1 of the ESI.†

2.3 Ellipsometry

Ellipsometry is a non-destructive, optical technique which is based on the detection of the change of polarization of light upon reflection from a substrate. Such a change is described by two parameters, ψ and Δ, which are related to the amplitude (E) and the phase (δ) of light by the following relations:

$$\tan\psi = \frac{\left|E_p^r\right|/\left|E_p^i\right|}{\left|E_s^r\right|/\left|E_s^i\right|} \quad (2)$$

$$\Delta = (\delta_p^r - \delta_s^r) - (\delta_p^i - \delta_s^i) \quad (3)$$

where the subscripts p, s indicate the parallel and perpendicular components of the light, while the superscripts i, r specify the incoming and reflected beam. The reflectivity properties of a sample can be expressed by the reflection coefficients, r_p and r_s,

$$r_p = \frac{\left|E_p^r\right|}{\left|E_p^i\right|} e^{i\left(\delta_p^r - \delta_p^i\right)} \quad (4)$$

$$r_s = \frac{\left|E_s^r\right|}{\left|E_s^i\right|} e^{i\left(\delta_s^r - \delta_s^i\right)} \quad (5)$$

whose combination with eqn (2) and (3) yield the fundamental equation of ellipsometry:

$$\tan\psi \cdot e^{i\Delta} = \frac{r_p}{r_s}. \quad (6)$$

The use of a proper layer model, which describes the system under measurement (substrate-film-medium) in terms of its optical properties (thickness d and refractive index n) can be obtained from the measured parameters Δ and ψ, which in turn describe the interaction between polarized light and sample. Specific literature is available on the topic to which the reader is addressed for a more detailed description of the technique.[55,56]

For the data analysis, the measured values of Δ and Ψ were fitted with a five box model consisting, from the bottom to the top, of (i) silicon substrate (n = 3.8850, $d = \infty$), (ii) silicon oxide (n = 1.46, d = 1.5 nm), (iii) initiator BTPAm monolayer (n = 1.50, d = 0.7 nm), (iv) polymer brushes ($n = n_{brush}$, $d = d_{brush}$), (v) liquid medium (n_{calc}, $d = \infty$). From the measured values of Δ and ψ, the corresponding combination of $n = n_{brush}$, $d = d_{brush}$ for the polymer brushes is obtained. The refractive index of solutions containing different urea concentrations was estimated by the empirical relations elaborated by Warren and Gordon[57] from experimental data on urea solutions. The corresponding values are reported in Table S2 of the ESI.† The degree of swelling ϕ_{sw} for PNIPAM brushes was calculated from the thickness d_{dry} of the dry brush and the thickness $d_{sw}(T)$ of the swollen brush at a given temperature T by

$$\phi_{sw} = \frac{d_{sw}(T) - d_{dry}}{d_{dry}} \times 100[\%]. \quad (7)$$

The brush collapse from the swollen conformation triggered by the increase of temperature was quantified from the difference between the measured thickness at $T > 288$ K and the initial value measured at 288 K:

$$\frac{d_{sw}(T) - d_{sw}(288\ \mathrm{K})}{d_{sw}(288\ \mathrm{K})} \times 100 = \frac{\Delta d_{sw}}{d_{sw}(288\ \mathrm{K})}[\%] \quad (8)$$

where d_{sw}(288 K) is the swollen brush thickness measured at 288 K and $d_{sw}(T)$ the PNIPAM thickness at temperatures $T > 288$ K. The transition temperature T_{tr} was taken as the temperature at half of the brush collapse.

Ellipsometry measurements were carried out using a Multiscope Null-Ellipsometer from Optrel GbR (Germany). The instrument is equipped with a red laser (λ = 632.8 nm) and a PCSA (polarizer–compensator–sample-analyzer) setup. For the measurements in dry condition, a home-built humidity cell was used, whose inside is flushed by nitrogen stream, reaching a value of (1.9 $\pm$ 0.1)% relative humidity. The angle of incidence was set to 70° and the sample was left drying for 20 minutes before measurements. For the measurements in liquid, the sample was soaked in a stainless steel cell filled with the urea solution. The instrument was equipped with light guides to drive the incident beam directly at the substrate/water interface and avoid the reflection at the liquid/air interface. Prior to the measurements, the sample was swollen in urea solution at 288 K for at least 2 h. A thermal cycle was applied by heating the liquid by means of a copper plate underneath the sample holder. The temperature of the liquid environment was measured continuously with a precision of $\Delta T = \pm 0.01$ K by means of a temperature sensor immersed in the sample cell.

2.4 Simulation details

A PNIPAM molecule with 24 monomers was studied by atomistic molecular dynamics (MD) simulations with the GROMACS 4.6.2 software package.[58–60] The force field parameters for PNIPAM presented in ref. 35 have been used to guarantee the occurrence of the coil-to-globule transition at temperatures below 328 K[34,35] while generalized AMBER force fields were used for urea.[61,62] Typical swollen and collapsed PNIPAM configurations have been obtained by using the original Metadynamics approach[63–65] as implemented within the PLUMED package.[66] We extracted the most swollen (radius of gyration R_g = 1.4 nm) and the collapsed state of PNIPAM (radius of gyration R_g = 0.8 nm) as found during the Metadynamics simulation and inserted them into cubic simulation boxes to study the influence of pure water, low and high aqueous urea

concentrations, respectively. The position of the backbone C_α carbon atoms have been kept fixed by using position restraints. We randomly inserted the corresponding number of urea and TIP3P water molecules[67] to model the required urea concentrations. In addition, we also simulated a PNIPAM molecule in pure water as a reference system. Electrostatic interactions for all systems have been calculated by the Particle Mesh Ewald method[68] and all bonds have been constrained by the LINCS algorithm.[69] First, we performed an energy minimization followed by a 2 ns warm-up run in a *NPT* ensemble at 288 K and 328 K with the Berendsen barostat and thermostat,[70] followed by *NPT* simulations of 20 ns for the production run with the same parameter sets. The minimum and maximum values for the length of the cubic simulation box are given by $\langle l \rangle_{\min}$ = 4.7 nm and $\langle l \rangle_{\max}$ = 6.49 nm in the *NPT* simulation depending on the system and the temperature. The corresponding effective urea concentrations for the different systems can be found in Table 1.

Hydrogen bonds were defined by a maximum distance criterion of 0.35 nm between acceptor and donor pairs with a maximum angle of 35°.

In fact, the study of polymer brushes is a challenging task for atomistic simulations. For the minimization of finite-size effects, a large number of grafted PNIPAM chains have to be considered which limits the applicability of atomistic approaches. In contrast, insights into polymer brush behavior can be provided by computationally efficient coarse-grained (CG) simulations[71] in which specific chemical details are usually neglected. Due to these reasons, CG approaches are not suitable for the detailed study of the PNIPAM–urea interactions such that we decided to simulate single PNIPAM molecules in an atomistic approach. The usage of restrained PNIPAM configurations was motivated by recent publications.[27,40] In fact, the simulation of PNIPAM coil-to-globule changes is a challenging task which might result in an insufficient sampling accuracy with regard to the interpretation of conformational transitions as rare events whose timescale usually exceeds the simulated time interval. Furthermore, the direct evaluation of free energy landscapes by free energy methods like metadynamics or umbrella sampling might also lead to wrong results due to inappropriate reaction coordinates and the presence of hysteresis effects.[72] Thus, the usage of restrained PNIPAM conformations as reference states avoids these drawbacks and provides a meaningful interpretation of the observed effects.[27,40]

Table 1 Average effective urea concentrations c_u for different restrained PNIPAM configurations defined by specific radii of gyration R_g and temperatures T in the *NPT* simulations. The following abbreviations are used to define the different combinations of urea concentration, polymer conformation and temperature: (l)ow or (h)igh urea concentration, (s)wollen or (c)ollapsed conformation, (288) and (328) for the simulation temperature

T [K]	R_g [nm]	c_u [mol L^{-1}]	Conformation	Label
288	0.8	0.5	Collapsed	lc288
328	0.8	0.5	Collapsed	lc328
288	1.4	0.5	Swollen	ls288
328	1.4	0.5	Swollen	ls328
288	0.8	6.1	Collapsed	hc288
328	0.8	4.8	Collapsed	hc328
288	1.4	6.1	Swollen	hs288
328	1.4	4.8	Swollen	hs328

2.5 Implications of the Kirkwood–Buff theory and local/bulk partition coefficients

The Kirkwood–Buff (KB) integral is given by

$$G_{\alpha\beta} = 4\pi \int_0^\infty r^2 \left(g_{\alpha\beta}^{\mu VT}(r) - 1 \right) \mathrm{d}r \tag{9}$$

in the limit of infinite distances with the radial distribution function $g_{\alpha\beta}(r)$ between molecular species α and β.[16,21,73–78] Since the full integration to infinite distances is not applicable for radial distribution functions obtained by computer simulations, the introduction of a cut-off radius is necessary.[76,79,80] Furthermore, as the Kirkwood–Buff integrals can be also identically evaluated in the *NpT* or *NVT* ensemble,[74,76] the equation above can be rewritten as

$$G_{\alpha\beta}(r_c) \approx 4\pi \int_0^{r_c} r^2 \left(g_{\alpha\beta}^{NpT}(r) - 1 \right) \mathrm{d}r \tag{10}$$

with the cut-off radius r_c.[77,79,80] The value of r_c = 1.8 nm was used for the data analysis, since the results of the radial distribution functions showed converged values from this point onwards. The physical meaning of Kirkwood–Buff integrals can be interpreted as the excess volume of a co-solute β around the central particle of a solute α, and they can be also used to study the local solvent accumulation behavior. In terms of notation, in the following description the solvent (water) will be denoted by the subscript α,β = '1', the solute (PNIPAM) by '2' and the osmolyte (urea) by '3'.

The preferential binding coefficient ν_{23} between PNIPAM and urea can be obtained from the difference of the KB integrals describing the distribution of water and urea around a PNIPAM chain, according to

$$\nu_{23} = \rho_3 (G_{23} - G_{21}) \tag{11}$$

where ρ_3 denotes the urea bulk number density. Note that the argument r_c for the KB integrals has been omitted. The preferential binding coefficient is connected with the transfer free energy

$$\Delta F_{23} = -RT\nu_{23} \tag{12}$$

with R the molar gas constant and T the temperature. The value for the transfer free energy estimates the amount of free energy which is needed to transfer a co-solute from the bulk to the surface of the solute.

The effects of osmolytes on macromolecular conformations can be evaluated in terms of the chemical equilibrium constant $K = \pi_s/\pi_c$ where π_s and π_c denote the fraction of PNIPAM molecules in the swollen (s) and the collapsed state (c). From the relation

$$\left(\frac{\partial \ln K}{\partial \ln a_3} \right) = \Delta\nu_{23} = \nu_{23}^s - \nu_{23}^c \tag{13}$$

the chemical activity of urea a_3 and the chemical equilibrium constant can be associated with the preferential binding

coefficients of urea to the swollen and the collapsed PNIPAM conformation (ν_{23}^{s} for the swollen and ν_{23}^{c} for the collapsed conformation).[76] The combination of eqn (13) with eqn (12) allows us to connect the chemical equilibrium in presence of osmolytes with the difference in the transfer free energy $\Delta\Delta F_{23}$,

$$\Delta\Delta F_{23} = \Delta F_{23}^{s} - \Delta F_{23}^{c} \quad (14)$$

to yield the final relation

$$\Delta\Delta F_{23} = -RT\left(\frac{\partial \ln K}{\partial \ln a_3}\right) \quad (15)$$

In accordance with the definition of the reaction constant K, it can be concluded that a change of the free energy can be associated with a change of the temperature if it is assumed that the free energy is mostly dominated by enthalpic contributions. Moreover, with regard to eqn (13), it can be also concluded, that the chemical equilibrium is shifted to the conformation with a stronger osmolyte accumulation.

Another robust parameter to study the osmolyte accumulation behavior is given by the local/bulk partition coefficient[40,81] according to

$$K_p(r) = \frac{(\langle n_u(r)\rangle/\langle n_w(r)\rangle)}{\left(n_u^{tot}/n_w^{tot}\right)} \quad (16)$$

where $\langle n_X(r)\rangle$ denotes the average number of water (X = w) or urea molecules (X = u) within a distance r and n_X^{tot} the total number of urea or water molecules in the simulation box. Thus, a preferential exclusion behavior leads to $K_p(r) < 1$ and a preferential binding of the osmolyte to $K_p(r) > 1$ at short distances r. Considering the local/bulk partition coefficient around the swollen PNIPAM configuration $K_p^s(r) = \exp(-\Delta F_p^s(r)/RT)$ and around the collapsed configuration $K_p^c(r) = \exp(-\Delta F_p^c(r)/RT)$, respectively, the local/bulk partition coefficient free energy difference can be expressed by

$$\Delta\Delta F_{K_p}(r) = -RT\log\left(\frac{K_p^s(r)}{K_p^c(r)}\right) \quad (17)$$

Eqn (17) implies that a negative value of $\Delta\Delta F_{K_p}(r)$ indicates a stronger accumulation of urea around the swollen state, and therefore the shift of the chemical equilibrium towards chain swelling, whereas a positive value reveals the stabilization of the collapsed conformation due to a stronger urea accumulation around the collapsed chain. Herewith, we exactly follow the implications given by eqn (13). Noteworthy, it can be also seen that even for negative preferential binding coefficients (eqn (11)) or local/bulk partition coefficients $K_p(r) > 1$, a shift of the chemical equilibrium for $\Delta\Delta F_{K_p}(r) \neq 0$ at short distances r can be observed, which is purely induced by the accumulation behavior of urea.

3 Results

3.1 Experimental results

The relative change of ellipsometric thickness $\Delta d_{sw}/d_{sw}(288\ K)$ calculated according to eqn (8) is reported in Fig. 1 as a function of temperature for different urea concentrations (c_u). Two important features in the obtained trends can be noticed: a shift of T_{tr} to lower values for increasing urea concentration c_u as denoted by the left arrow, and a weaker brush collapse in urea solutions compared to pure water as denoted by the right arrow. The weaker brush collapse above the transition temperature at high urea concentrations can be discussed with the arguments given by Cremer and co-workers in ref. 38, where increasing PNIPAM radii observed at increasing urea concentration were explained by bridging effects of the osmolyte in order to cross-link PNIPAM chains. An analogous effect in this case might be responsible for the reduced brush collapse at high c_u. In order to analyze the effects of urea on the thermal behavior of PNIPAM in more detail, T_{tr} and ϕ_{sw} were extracted from the ellipsometry curves. The values of T_{tr} for PNIPAM brushes in presence of different urea concentrations are presented in Fig. 2. A systematic decrease of T_{tr} for increasing urea concentrations was found, with the evidence of two distinct regimes: a low concentration regime between 0 and 0.5 mol L^{-1}, with a linear decrease of T_{tr} as a function of c_u (inset in Fig. 2), and a high urea concentration regime between 2 and 7 mol L^{-1} with a weaker, but constant decrease of T_{tr}. Two distinct regimes, although not so noticeable, were found also for single PNIPAM chains.[38] Thus, it can be concluded that this effect is not exclusively characteristic for PNIPAM brushes and it demonstrates that molecular PNIPAM–urea interactions dominate the chain behavior, independent of the system geometry. This allows us to apply the knowledge of single chain–urea interactions to more complex and crowded molecular systems, like polymer brushes, which might be of paramount importance for the application of grafted biomolecular (*e.g.* proteins) systems.[71]

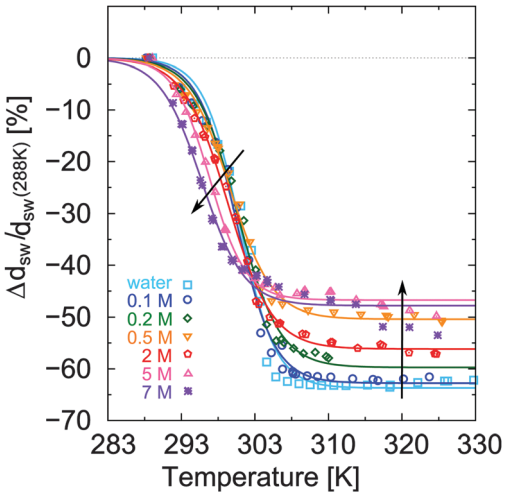

Fig. 1 Relative thickness change, $\Delta d_{sw}/d_{sw}(288\ K)$, as a function of temperature measured in urea solution at different molar concentration. The lines are the fit of a sigmoid on the experimental data and are traced as a guide for the eye. Arrows indicate the effect of added urea.

Remarkably, the influence of urea on the transition temperature of PNIPAM may have different origins:[36] on the one hand, the presence of urea changes the properties of the aqueous medium;[29] on the other hand, the osmolyte could

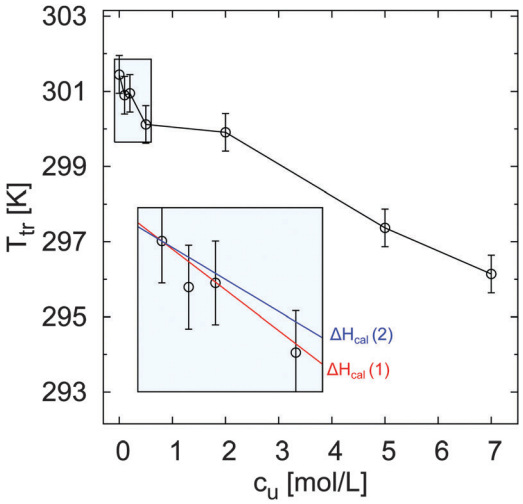

Fig. 2 Transition temperature T_{tr} of PNIPAM brushes as a function of urea concentration. The samples were subjected to a heating cycle from 288 K to 328 K. The values T_{tr} can be related to the temperature where half of the brush is collapsed. The inset in the plot reports the values of T_{tr} between 0 and 0.5 mol L^{-1}, while the straight lines describe the calculated trends according to eqn (18) for the calorimetric enthalpy $\Delta H_{cal}(1)$ = 5.5 kJ mol^{-1} and $\Delta H_{cal}(2)$ = 7 kJ mol^{-1} reported for the NIPAM dehydration in water.

directly interact with the polymer, as recently demonstrated for high urea concentrations.[38,82]

While at high c_u the direct urea binding to the polymer is very likely, it is important to verify which mechanism dominates the change of T_{tr} for a PNIPAM brush in presence of a low molar urea concentration. As a first hypothesis, it is assumed that urea does not directly interact with PNIPAM, *i.e.* it is preferentially excluded from a PNIPAM surface. Under this condition, the shift of T_{tr} might be reasoned by a change of the PNIPAM hydration properties.

From the decrease of the chemical potential of bulk water upon addition of urea, and from the equilibrium condition at T_{tr} with identical chemical potentials for H_2O (bulk) and H_2O (brush) phase, the following relation between the temperature shift ΔT_{tr} and the dehydration enthalpy ΔH_{dehy} can be derived:

$$\Delta T_{tr} = -\frac{R\left(T_{tr}^{0}\right)^{2}}{\Delta H_{dehy}}\chi_u \qquad (18)$$

where T_{tr}^{0} is the transition temperature in pure water (c_u = 0 mol L^{-1}), ΔH_{dehy} corresponds to the dehydration enthalpy per mole of water and χ_u denotes the urea–water mole fraction. The full derivation of this relation is given in the ESI.† It has to be noted that a similar expression was also derived in ref. 22.

It is worth to mention that this approach represents a simplified picture of the system, where the transition enthalpy of the macromolecule from swollen to collapsed state is omitted. The validity of eqn (18) to describe the experimental data of Fig. 2 at low c_u would confirm the dilution effect of bulk water by urea, *i.e.* indirect effects. Previous studies on the coil-to-globule transition of PNIPAM reported calorimetric enthalpy values ΔH_{cal} between 5.5 and 7 kJ mol^{-1} for a single (NIPAM) repeating unit.[83,84] This can be related to the release of one bound water molecule from each monomer unit, in agreement with previous experimental results.[83,85] Other literature works report the release of a much higher number of water molecules per NIPAM unit in bulk or in gels.[86,87] Nevertheless, in our evaluation only the water molecules directly bound to the monomer unit *via* H-bonding are considered.

Assuming that the same process occurs for the dehydration of PNIPAM brushes in presence of low molar urea concentrations, where direct urea–PNIPAM interactions are negligible, it follows that $\Delta H_{cal} \sim \Delta H_{dehy}$ and therefore it is possible to calculate the theoretical trend of ΔT_{tr} as a function of c_u for the reported dehydration enthalpies of $\Delta H_{cal}(1)$ = 5.5 kJ mol^{-1} and $\Delta H_{cal}(2)$ = 7 kJ mol^{-1}. The corresponding functions are shown as solid lines in the inset of Fig. 2. The agreement between experimental data and theoretical trends corroborates the assumption that the dehydration mechanism of PNIPAM in low concentrated urea solutions is comparable to the dehydration in pure water in accordance to ref. 83 and 84. Thus, the shift of the transition temperature can be explained by the dilution of water by urea as induced by the mole fraction χ_u.

A different mechanism is likely to occur in the high concentration regime, where urea is known to have a significant influence on the stability of proteins and a direct osmolyte–polymer binding has been reported in previous studies.[38,82] Indeed, the profile of T_{tr} shown in Fig. 2 is very similar to the results presented by Cremer and coworkers[38] obtained by Fourier transformed infrared (FTIR) spectroscopy measurements. The reported FTIR data showed a strong amide band for PNIPAM in 6 M urea solution, with a major contribution from C═O(PNIPAM)–H_2O hydrogen bonds and a second minor one from C═O(PNIPAM)–NH(urea) bonds. An analogous effect is likely to dominate the collapse of PNIPAM brushes at $c_u \geq 2$ M, as indicated by our results, where the direct binding of urea with (NIPAM) monomers might introduce the aggregation of adjacent chains, such that urea acts as a cross-linking agent.[38] Evidence of direct polymer–osmolyte binding was also found by Wang *et al.*[82] for poly(*N*,*N*-dimethylacrylamide) (PDMA) and poly(*N*,*N*-diethylacrylamide) (PDEA) brushes by atomic force microscopy-based single molecule force spectroscopy (SMFS). The enhanced stiffness of the polymer chains in presence of 2 M and 8 M urea solution was explained by the formation of hydrogen bonds between the polymer side groups and urea molecules. Cross-linking of urea *via* hydrogen bonding was also reported by Lu *et al.*[88] to explain urea-induced aggregation of PNIPAM chains observed by static and dynamic light scattering. According to Cremer and co-workers,[32,38] a schematic representation of the bridging mechanism between PNIPAM chains in presence of urea is shown in Fig. 3. This aspect will be discussed in more detail in the next section.

To study the effect of urea on the conformation of grafted chains, the swelling degree ϕ_{sw} of PNIPAM brushes below (288 K) and above (328 K) the phase transition temperature was calculated according to eqn (7) for the different urea concentrations. As it is shown in Fig. 4, a stronger swelling percentage compared to pure water (c_u = 0 mol L^{-1}) is achieved

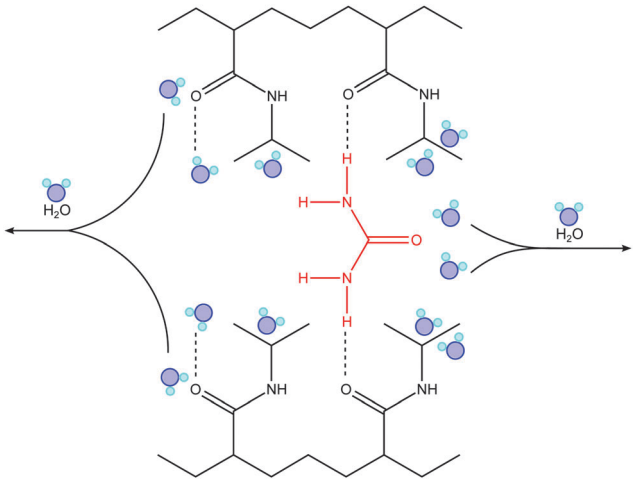

Fig. 3 Schematic representation of the urea bridging effect between adjacent PNIPAM chains occurring in the high concentration regime ($c_u \geq 2$ M). Urea as a cross-linking agent significantly enhances the stability of the collapsed state. The image was inspired by ref. 32 and 38.

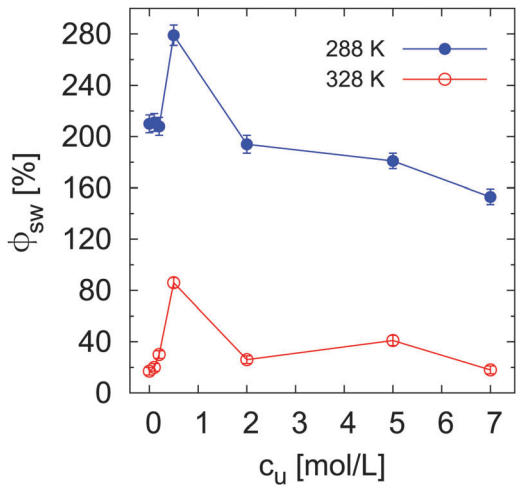

Fig. 4 Swelling degree ϕ_{sw} of PNIPAM brushes at 288 K and 328 K for different urea concentrations. The parameter ϕ_{sw} was calculated according to eqn (7).

for low urea concentrations both at 288 K and 328 K. In contrast, in the high concentration regime ($c_u \geq 2$ mol L^{-1}) ϕ_{sw} is lower (288 K) or similar (328 K) to the swelling degree in pure water. Analogous to the previous assumption, we rule out a strong accumulation of urea inside the brush. Therefore indirect effects might be responsible for the observed enhancement of brush swelling at c_u = 0.5 mol L^{-1}. More specifically, steric effects on the chain conformation due to the presence of urea in the swelling medium might lead to higher chain stretching. This aspect is analyzed and clarified by the numerical studies presented in the next section. It is worth to mention that this effects might not be visible at concentrations below 0.5 M due to the very low amount of the osmolyte in the swelling medium. In the case of high c_u, there are two important implications: at low temperature, increasing urea concentrations decrease the brush swelling, likely due to a decrease of water bonding (lower hydration) to the polymer chain; at high temperature, the presence of urea molecules around the macromolecule might be responsible for the stabilization of the collapsed state. It has to be noticed that the considered temperatures of 288 K and 328 K are significantly below and above the transition temperature, such that temperature dependent dehydration effects, which could in principle influence T_{tr}, can be omitted.

An analogous representation of the structural transition of PNIPAM brushes across T_{tr} is given by the percentage of the total brush collapse (*i.e.* reached at 328 K), which is reported in the ESI.† The obtained trend as a function of c_u demonstrates a reduced brush collapse for any urea concentration compared to pure water. While in the high concentration regime this can be reasonably explained by the reduced water content in the brush, which would confirm the direct polymer–urea interaction reported by other authors,[38] in the low concentration regime it is likely the result of a more subtle interplay between hydration properties and bulk effects of urea.

In summary, the experimental results indicate concentration-dependent properties of urea on transition temperatures and resulting conformations of PNIPAM brushes above and below T_{tr}. The understanding of the molecular origins of the observed effects on phase transition and swelling behavior motivated the numerical studies presented in the next subsection. Herewith, we mostly focus on the interactions between PNIPAM, water and urea in the low/high concentration regimes and below/above the phase transition temperature.

3.2 Numerical results

The interpretation of the experimental results presented in the previous section suffer of some speculative hypotheses to deduce a suitable molecular mechanism to explain the observed effects. This is an intrinsic limitation of most experimental methods, but as we demonstrated in a previous publication,[89] it can be overcome when experiments and simulations are interpreted in a synergistic way. Following this approach, simulation results are presented to complement the experimental findings and to validate their interpretation.

Typical snapshots of a collapsed and a swollen PNIPAM configuration in a low molar urea solution are presented in Fig. 5. By introducing specific position restraints to fix the PNIPAM configurations, it was possible to avoid transitions into metastable states and to obtain reliable and well-sampled statistically averaged values. A detailed discussion of this approach is given in the section Simulation details.

In order to study the hydration behavior, the local Kirkwood–Buff integrals $G_{21}(r)$ for PNIPAM and water molecules at 288 K for c_u = 0.5 mol L^{-1} were calculated. The values for $G_{21}(r)$ in pure water were also estimated for comparison. The results are presented at the top of Fig. 6. Only small differences between the $G_{21}(r)$ in urea solution and the value in pure water can be observed. Hence, it becomes clear that low molar urea concentrations lead to a weak change in the PNIPAM hydration behavior at low temperatures, as it was also concluded from the experimental results.

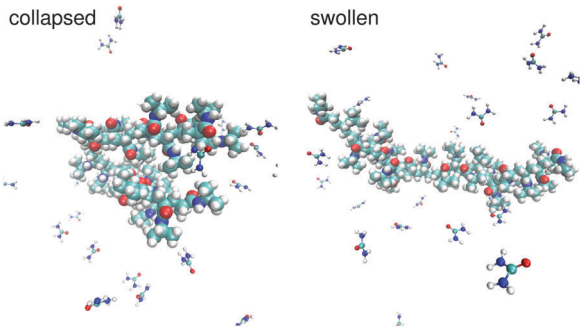

Fig. 5 Typical simulation snapshots of PNIPAM in presence of a low molar urea solution at 288 K. The snapshot on the left side represents a collapsed PNIPAM configuration with a radius of gyration of 0.8 nm whereas the right side shows a swollen configuration with a radius of gyration of 1.4 nm. Both conformations have been used for the study of the hydration and the urea binding properties.

Changes in the PNIPAM–water interactions in presence of urea can be easily evaluated considering the differences of the Kirkwood–Buff integrals according to

$$\Delta G_{21} = G_{21}^{u} - G_{21}^{w} \quad (19)$$

with G_{21}^{w} for pure water and G_{21}^{u} in presence of urea. The corresponding results at r_c = 1.8 nm for all investigated combinations of chain conformation, urea concentration and temperature are shown at the bottom of Fig. 6. Larger values of ΔG_{21} were observed for all systems at 328 K and in particular for the swollen conformations (ls328 and hs328). In contrast, a slightly modified water accumulation behavior is evident for all systems at 288 K. It can be therefore concluded that at low temperature the presence of urea only weakly perturbs the water structure around PNIPAM, in good agreement with previous assumptions in the literature[2,20] where it was discussed that urea can be well integrated into the water structure network.

To study the direct and local interactions between PNIPAM and urea or water molecules, the number of hydrogen bonds was calculated. The corresponding results and further findings are shown in Fig. 7 and in Table S3 of the ESI.† At low molar urea concentrations, the number of water–PNIPAM hydrogen bonds is comparable to pure water (ΔH-bonds (water)) for both temperatures (ls288, lc288, ls328 and lc328). This means that the first solvent shell around PNIPAM at low c_u has a similar composition as in pure water, and only a small number of urea–PNIPAM hydrogen bonds (H-bonds (urea)) are formed. These results validate the previous assumptions of a minor PNIPAM–urea interaction in presence of low c_u, and support the hypothesis of indirect effects from the water–urea network on the chain conformation at low c_u.

In contrast, a significant decrease of water hydrogen bonds compared to pure water (ΔH-bonds (water)) is found at high c_u (hs288, hc288, hs328 and hc328), and also the total number of hydrogen bonds is smaller compared with pure water (*i.e.* large negative values of ΔH-bonds (total)). Interestingly, at high temperature (hs328 and hc328) the number of urea hydrogen bonds even exceeds the number of water hydrogen bonds

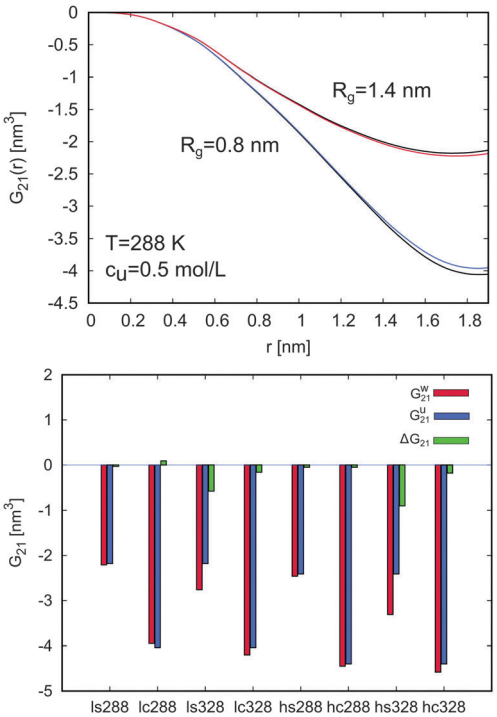

Fig. 6 Top: Kirkwood–Buff integrals $G_{21}(r)$ for water molecules around the swollen (R_g = 1.4 nm: red and upper black line) and the collapsed PNIPAM configuration (R_g = 0.8 nm: blue and lower black line) in a 0.5 M urea solution and pure water at 288 K. The black lines represent the Kirkwood–Buff integral values around the swollen and the collapsed configuration in pure water, while the blue and the red line correspond to the values for water molecules in a 0.5 M urea solution. Bottom: Values for the Kirkwood–Buff integrals G_{21} at r_c = 1.8 nm for water molecules around all considered PNIPAM configurations and system parameters (288 K and 328 K, (h)igh and (l)ow molar urea concentrations, (s)wollen and (c)ollapsed PNIPAM configuration). The red bars for G_{21}^{w} denote the values in pure water, the blue bars for G_{21}^{u} represent the values in presence of urea, and the green bars for ΔG_{21} correspond to the difference in the KB integrals according to eqn (19).

(H-bonds (urea) > H-bonds (water)) meaning that in this condition urea replaces water at molecular interfaces.[88] Moreover, from the data reported in Table S3 of the ESI† it can be seen that urea hydrogen bonds are energetically stronger than water hydrogen bonds. From these results it can be concluded that at high c_u urea binding dominates the behavior of PNIPAM chains across the phase transition, while the effects arising from the change of PNIPAM–water interactions are negligible.

In order to classify the hydrogen bonds with respect to their related energetic contributions according to the transition state theory with the Luzar–Chandler approach,[90,91] it is possible to calculate the forward rate constants k of hydrogen bonds *via* $k \sim \exp(-\Delta F^{*}/k_B T)$, where ΔF^{*} denotes the activation free binding energy. The corresponding values for water–PNIPAM and urea–PNIPAM hydrogen bonds are shown in Table S3 of the ESI.† The most relevant result is the decrease of the activation free energies of water for increasing urea concentrations. The replacement of water–PNIPAM hydrogen bonds with urea–PNIPAM hydrogen bonds is therefore energetically favorable. Furthermore, for increasing urea concentration, the strength of

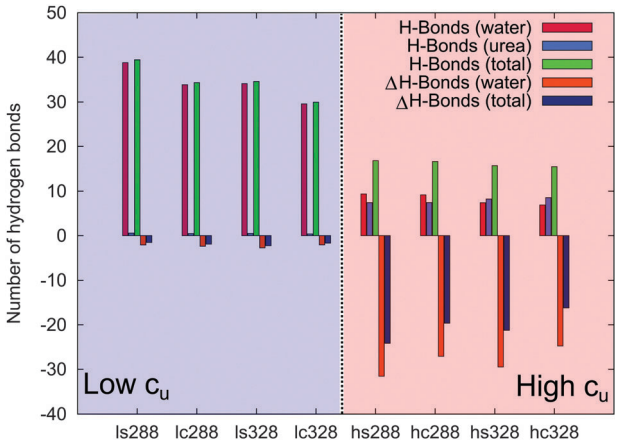

Fig. 7 Number of PNIPAM hydrogen bonds in urea solutions with urea (H-bonds (urea)), water (H-bonds (water)), total number of hydrogen bonds (H-bonds (total)) and the difference of H-bonding for the same configuration and temperature in pure water (ΔH-bonds (water) and ΔH-bonds (total)).

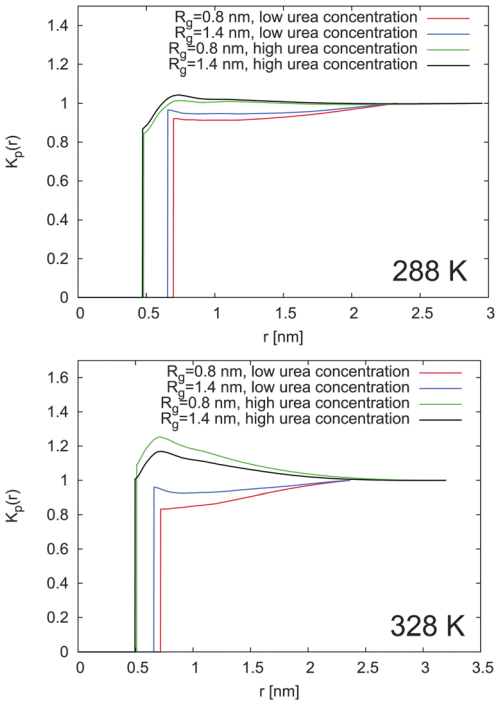

Fig. 8 Local partition coefficient for swollen (R_g = 1.4 nm) and collapsed (R_g = 0.8 nm) PNIPAM conformations in presence of high and low molar urea concentrations at 288 K (top) and at 328 K (bottom).

water hydrogen bonds is slightly lowered, which facilitates the release of water molecules from the first solvent shell, in agreement with the experimental results (Fig. 2). Moreover, the increasing amount of urea molecules favors PNIPAM dehydration also due to the replacement of water by urea in the first solvent shell. These conclusions are additionally supported by the stagnating values of ϕ_{sw} at high urea concentrations (Fig. 4).

In order to evaluate the influence of urea binding on the shift of the chemical equilibrium towards the swollen or the collapsed state, the local/bulk partition coefficients were estimated according to eqn (16). The results reported in Fig. 8 prove that the local/bulk partition coefficients $K_p(r)$ for low c_u at both temperatures are smaller than 1 at all distances. This confirms that urea is preferentially excluded from the PNIPAM backbone at low concentrations, in perfect agreement with the small number of urea–PNIPAM hydrogen bonds reported in Fig. 7. The highly stretched PNIPAM conformations observed at low urea concentrations (c_u = 0.5 mol L^{-1}) in Fig. 4 can be therefore attributed to the weaker urea exclusion around the swollen conformation in accordance to eqn (13). Although urea is very poorly bound to PNIPAM, the interaction with the water molecules around the macromolecule leads to volume exclusion effects, which contribute to enhance the chain stretching. The swollen conformation is therefore more favored compared to the collapsed state. A slightly stronger urea accumulation at short distances ($r \leq 1$ nm) is found for high c_u, which is more pronounced at high temperature, and demonstrates the preferential binding of urea to PNIPAM chains. However, the preferential exclusion of urea for low c_u results in a slight dehydration, as demonstrated by the water accumulation behavior according to the KB integrals presented in Fig. 6 and the negative values for ΔH-bonds (water). This finding is in good agreement with the general explanation for the occurrence of a coil to globule transition for PNIPAM[33–35] and the shift to lower transition temperatures. It can be assumed that urea molecules are preferentially excluded from PNIPAM at low c_u where it is energetically unfavorable to replace water with urea molecules. The situation changes for high c_u at high temperature, where a significant dehydration upon phase transition occurs and the strong binding of urea molecules is energetically favorable to compensate the loss of the water molecules. These two mechanisms are able to explain the two different slopes for the decrease of the transition temperature observed for different urea concentrations in Fig. 3.

The shift of the chemical equilibrium towards swollen or collapsed PNIPAM conformations as shown in Fig. 4 can be rationalized with regard to the local/bulk partition coefficient free energy difference (eqn (17)). It becomes obvious that only the high molar urea concentration at 328 K indicates a positive value of $\Delta\Delta F_{K_p} \approx 0.2$ kJ mol^{-1} at a PNIPAM distance of r = 0.5 nm, which validates the energetic stability of the collapsed PNIPAM conformation. For all the other temperatures and concentrations, swollen conformations are preferred. Based on these findings, it can be concluded that the chemical equilibrium is slightly shifted towards the more swollen conformations for low c_u at both temperatures, in agreement with the experimental results (Fig. 4), whereas only high temperatures and high c_u induce a shift of the chemical equilibrium towards the collapsed state. The strong attraction of urea to PNIPAM in high concentrated solutions and at high temperatures may rationalize the previously discussed effects for urea in terms of a cross-linking agent between adjacent PNIPAM chains[27,32,38,40,88] above a critical urea concentration. The presence of a direct urea binding can be also assumed with regard to the stagnating values for ϕ_{sw} at $c_u \geq 2$ mol L^{-1} which can be rationalized by a fully saturated urea shell around PNIPAM.

4 Summary and conclusions

In this work, the effect of urea on the conformational behavior of PNIPAM brushes was studied by combining optical experiments and atomistic molecular dynamics simulations. The reported results indicated a concentration-dependent binding behavior between urea and PNIPAM. In the low concentration regime ($c_u \leq 0.5$ mol L^{-1}), urea is preferentially excluded from the PNIPAM backbone. Hence, the linear decrease of T_{tr} was rationalized by indirect effects of urea, which influence the dehydration process at high temperature by dilution of bulk water. However, despite the low number of urea molecules around PNIPAM in the first solvent shell, it was found that a more stretched conformation is stabilized due to a more favorable urea accumulation around the swollen conformation and excluded volume effects, as a consequence of the water–urea network around the macromolecule.[92] In contrast, in the high concentration regime a preferential binding of urea to PNIPAM was found at both temperatures. Due to the small number of water molecules bound to PNIPAM, it can be assumed that the shift of the transition temperatures at high c_u is mostly dominated by direct urea interactions with PNIPAM. Moreover, the high positive local/bulk partition coefficient of urea at 328 K supports the hypothesis of urea acting as a crosslinking agent between adjacent PNIPAM chains.[32,38,88]

Thus, two basic mechanisms for different urea concentrations are proposed: (1) a preferential exclusion of urea from PNIPAM surface at low molar concentrations. This was rationalized by the experimental results, which supported a similar dehydration mechanism at low c_u as in pure water, proving the absence of a direct binding; (2) a preferential binding of urea to PNIPAM above a critical concentration ($c_u \geq 2$ mol L^{-1}). This produces a further decrease of the transition temperature in agreement to previous findings,[38,82] and a cross-linking effect due to a favorable binding between adjacent chains with a similar mechanism as proposed earlier.[38,88] Although several differences between numerical and experimental studies exist, for instance the consideration of a single chain in contrast to polymer brushes, a reasonable agreement between the results was found. This qualitative coincidence is of crucial importance, as it demonstrates that the experimental outcomes are strongly influenced by single chain properties and not by collective effects of the brush. Specific effects like cross-linking between the polymer chains which have been reported for high urea concentrations[38,88] are not detectable by the simulations. However, indirect hints were found, like the strong accumulation of urea molecules around PNIPAM chains by a preferential binding mechanism, providing a reasonable explanation of the experimental observations. With regard to the two distinct accumulation regimes of urea, it has to be mentioned that explicit reasons for a similar behavior have been also recently discussed,[22] and with regard to charged co-solutes, the presence of specific binding mechanisms for chaotropic ions was demonstrated.[93,94]

In conclusion, the conformational behavior and the transition temperatures of PNIPAM brushes are strongly affected by the presence of urea, either by indirect effects or by direct polymer–osmolyte interactions. This article demonstrates that the combined results of experiments and simulations point towards the most reliable methodology to study molecular mechanisms and their consequences for macromolecular conformations.

Acknowledgements

The authors greatly acknowledge helpful discussions with Anand Narayanan Krishnamoorthy, Ewa Anna Oprzeska-Zingrebe, Nico van der Vegt, Francisco Rodriguez-Ropero, Jan Heyda, Dominik Horinek and Pavel Jungwirth. The authors J. S., J. M. and C. H. thank the Deutsche Forschungsgemeinschaft through the cluster of excellence initiative 'Simulation Technology' (EXC 310) and the SFB 716 for financial support. M. A. S. thanks the excellence cluster ''The Hamburg Centre for Ultrafast Imaging – Structure, Dynamics, and Control of Matter at the Atomic Scale'' of the DFG. The authors S. M. and R. v. K. acknowledge the International graduate School IRTG 1524 (DFG) for the financial support.

References

1 P. H. Yancey, *J. Exp. Biol.*, 2005, **208**, 2819–2830.
2 D. R. Canchi and A. E. Garca, *Annu. Rev. Phys. Chem.*, 2013, **64**, 273–293.
3 D. Harries and J. Rösgen, *Methods Cell Biol.*, 2008, **84**, 679–735.
4 R. Politi and D. Harries, *Chem. Commun.*, 2010, **46**, 6449–6451.
5 B. J. Bennion and V. Daggett, *Proc. Natl. Acad. Sci. U. S. A.*, 2003, **100**, 5142–5147.
6 R. Zangi, R. Zhou and B. Berne, *J. Am. Chem. Soc.*, 2009, **131**, 1535–1541.
7 D. A. Beck, B. J. Bennion, D. O. Alonso and V. Daggett, *Methods Enzymol.*, 2007, **428**, 373–396.
8 A. M. Bhattacharyya and P. Horowitz, *J. Biol. Chem.*, 2000, **275**, 14860–14864.
9 A. K. Bhuyan, *Biochemistry*, 2002, **41**, 13386–13394.
10 M. A. Schroer, M. Paulus, C. Jeworrek, C. Krywka, S. Schmacke, Y. Zhai, D. C. F. Wieland, C. J. Sahle, M. Chimenti, C. A. Royer, B. Garcia-Moreno, M. Tolan and R. Winter, *Biophys. J.*, 2010, **99**, 3430–3437.
11 M. A. Schroer, Y. Zhai, D. C. F. Wieland, C. J. Sahle, J. Nase, M. Paulus, M. Tolan and R. Winter, *Angew. Chem., Int. Ed.*, 2011, **50**, 11413–11416.
12 J. Smiatek, R. K. Harishchandra, O. Rubner, H.-J. Galla and A. Heuer, *Biophys. Chem.*, 2012, **160**, 62–68.
13 J. Smiatek, R. K. Harishchandra, H.-J. Galla and A. Heuer, *Biophys. Chem.*, 2013, **180**, 102–109.
14 R. K. Harishchandra, S. Wulff, G. Lentzen, T. Neuhaus and H.-J. Galla, *Biophys. Chem.*, 2010, **150**, 37–46.
15 K. D. Collins, G. W. Neilson and J. E. Enderby, *Biophys. Chem.*, 2007, **128**, 95–104.
16 D. Horinek and R. R. Netz, *J. Phys. Chem. A*, 2011, **115**, 6125–6136.

17 E. Schneck, D. Horinek and R. R. Netz, *J. Phys. Chem. B*, 2013, **117**, 8310–8321.
18 A. Narayanan Krishnamoorthy, C. Holm and J. Smiatek, *J. Phys. Chem. B*, 2014, **118**, 11613–11621.
19 K. D. Collins, *Biophys. J.*, 1997, **72**, 65–76.
20 K. D. Collins, *Methods*, 2004, **34**, 300–311.
21 J. Smiatek, *J. Phys. Chem. B*, 2014, **118**, 771–782.
22 J. Heyda and J. Dzubiella, *J. Phys. Chem. B*, 2014, **118**, 10979–10988.
23 W. Lim, J. Roesgen and S. Englander, *Proc. Natl. Acad. Sci. U. S. A.*, 2009, **106**, 2595–2600.
24 J. Dunbar, H. P. Yennawar, S. Banerjee, J. Luo and G. K. Farber, *Protein Sci.*, 1997, **6**, 1727–1733.
25 E. P. O'Brien, R. I. Dima, B. Brooks and D. Thirumalai, *J. Am. Chem. Soc.*, 2007, **129**, 7346–7353.
26 T. Street, D. Bolen and G. Rose, *Proc. Natl. Acad. Sci. U. S. A.*, 2006, **103**, 17064–17065.
27 F. Rodriguez-Ropero and N. F. A. van der Vegt, *Phys. Chem. Chem. Phys.*, 2015, **17**, 8491–8498.
28 R. Breslow and T. Guo, *Proc. Natl. Acad. Sci. U. S. A.*, 1990, **87**, 167–169.
29 S. N. Timasheff, *Biochemistry*, 1992, **31**, 9857–9864.
30 E. I. Tiktopulo, V. N. Uversky, V. B. Lushchik, S. I. Klenin, V. E. Bychkova and O. B. Ptitsyn, *Macromolecules*, 1995, **28**, 7519–7524.
31 G. Graziano, *Int. J. Biol. Macromol.*, 2000, **27**, 89–97.
32 Y. Zhang and P. S. Cremer, *Annu. Rev. Phys. Chem.*, 2010, **61**, 63–83.
33 S. A. Deshmukh, S. K. Sankaranarayanan, K. Suthar and D. C. Mancini, *J. Phys. Chem. B*, 2012, **116**, 2651–2663.
34 H. Du, S. R. Wickramasinghe and X. Qian, *J. Phys. Chem. B*, 2013, **117**, 5090–5101.
35 H. Du, R. Wickramasinghe and X. Qian, *J. Phys. Chem. B*, 2010, **114**, 16594–16604.
36 C. Hofmann and M. Schönhoff, *Colloid Polym. Sci.*, 2009, **287**, 1369–1376.
37 C. H. Hofmann and M. Schönhoff, *Colloid Polym. Sci.*, 2012, **290**, 689–698.
38 L. B. Sagle, Y. Zhang, V. A. Litosh, X. Chen, Y. Cho and P. S. Cremer, *J. Am. Chem. Soc.*, 2009, **131**, 9304–9310.
39 E. A. Algaer and N. F. van der Vegt, *J. Phys. Chem. B*, 2011, **115**, 13781–13787.
40 F. Rodriguez-Ropero and N. F. van der Vegt, *J. Phys. Chem. B*, 2014, **118**, 7327–7334.
41 Y. Gao, J. Yang, Y. Ding and X. Ye, *J. Phys. Chem. B*, 2014, **118**, 9460–9466.
42 Y. Fang, J.-C. Qiang, D.-D. Hu, M.-Z. Wang and Y.-L. Cui, *Colloid Polym. Sci.*, 2001, **279**, 14–21.
43 L. Liu, Y. Shi, C. Liu, T. Wang, G. Liu and G. Zhang, *Soft Matter*, 2014, **10**, 2856–2862.
44 K. Fuchise, R. Kakuchi, S.-T. Lin, R. Sakai, S.-I. Sato, T. Satoh, W.-C. Chen and T. Kakuchi, *J. Polym. Sci., Part A: Polym. Chem.*, 2009, **47**, 6259–6268.
45 M. A. C. Stuart, W. T. S. Huck, J. Genzer, M. Müller, C. Ober, M. Stamm, G. B. Sukhorukov, I. Szleifer, V. V. Tsukruk, M. Urban, F. Winnik, S. Zauscher, I. Luzinov and S. Minko, *Nat. Mater.*, 2010, **9**, 101–113.
46 J. Gensel, T. Borke, N. P. Pérez, A. Fery, D. V. Andreeva, E. Betthausen, A. H. E. Müller, H. Möhwald and E. V. Skorb, *Adv. Mater.*, 2012, **24**, 985–989.
47 P. Akkahat and V. P. Hoven, *Colloids Surf., B*, 2011, **86**, 198–205.
48 K. Matyjaszewski and J. Xia, *Chem. Rev.*, 2001, **101**, 2921–2990.
49 P. Laurent, G. Souharce, J. Duchet-Rumeau, D. Portinha and A. Charlot, *Soft Matter*, 2012, **8**, 715–725.
50 L. C. H. Moh, M. D. Losego and P. V. Braun, *Langmuir*, 2011, **27**, 3698–3702.
51 S. Sanjuan, P. Perrin, N. Pantoustier and Y. Tran, *Langmuir*, 2007, **23**, 5769–5778.
52 S. Christau, T. Möller, Z. Yenice, J. Genzer and R. von Klitzing, *Langmuir*, 2014, **30**, 13033–13041.
53 X. Lu, L. Zhang, L. Meng and Y. Liu, *Polym. Bull.*, 2007, **59**, 195–206.
54 J. Xia and K. Matyjaszewski, *Macromolecules*, 1997, **30**, 7697–7700.
55 J. B. Theeten and D. E. Aspnes, *Annu. Rev. Mater. Sci.*, 1981, **11**, 97–122.
56 *Handbook of Ellipsometry*, ed. H. G. Tompkins and E. A. Irene, William Andrew, Inc., Norwich, 2005, vol. 30, pp. 1–902.
57 J. R. Warren and J. A. Gordon, *J. Biol. Chem.*, 1970, **245**, 4097–4104.
58 D. V. D. Spoel, E. Lindahl, B. Hess, G. Groenhof, A. E. Mark and H. J. C. Berendsen, *J. Comput. Chem.*, 2005, **26**, 1701–1718.
59 H. J. C. Berendsen, D. van der Spoel and R. van Drunen, *Comput. Phys. Commun.*, 1995, **91**, 43–56.
60 S. Pronk, S. Páll, R. Schulz, P. Larsson, P. Bjelkmar, R. Apostolov, M. R. Shirts, J. C. Smith, P. M. Kasson, D. van der Spoel, B. Hess and E. Lindahl, *Bioinformatics*, 2013, **29**, 845–854.
61 J. Wang, R. M. Wolf, J. W. Caldwell, P. A. Kollman and D. A. Case, *J. Comput. Chem.*, 2004, **25**, 1157–1174.
62 J. Wang, W. Wang, P. A. Kollman and D. A. Case, *J. Mol. Graphics Modell.*, 2006, **25**, 247–260.
63 A. Laio and M. Parrinello, *Proc. Natl. Acad. Sci. U. S. A.*, 2002, **99**, 12562–12566.
64 A. Laio and F. L. Gervasio, *Rep. Prog. Phys.*, 2008, **71**, 126601.
65 J. Smiatek and A. Heuer, *J. Comput. Chem.*, 2011, **32**, 2084–2096.
66 M. Bonomi, D. Branduardi, G. Bussi, C. Camilloni, D. Provasi, P. Raiteri, D. Donadio, F. Marinelli, F. Pietrucci and R. A. Broglia, *Comput. Phys. Commun.*, 2009, **180**, 1961–1972.
67 W. L. Jorgensen, J. Chandrasekhar, J. D. Madura, R. W. Impey and M. L. Klein, *J. Chem. Phys.*, 1983, **79**, 926–935.
68 T. Darden, D. York and L. Pedersen, *J. Chem. Phys.*, 1993, **98**, 10089–10092.
69 B. Hess, H. Bekker, H. J. C. Berendsen and J. G. E. M. Fraaije, *J. Comput. Chem.*, 1997, **18**, 1463–1472.
70 H. J. Berendsen, J. P. M. Postma, W. F. van Gunsteren, A. DiNola and J. Haak, *J. Chem. Phys.*, 1984, **81**, 3684–3690.
71 J. Smiatek, A. Heuer, H. Wagner, A. Studer, C. Hentschel and L. Chi, *J. Chem. Phys.*, 2013, **138**, 044904.

72 J. Smiatek, D. Janssen-Müller, R. Friedrich and A. Heuer, *Physica A*, 2014, **394**, 136–144.
73 J. G. Kirkwood and F. P. Buff, *J. Chem. Phys.*, 1951, **19**, 774–777.
74 A. Y. Ben-Naim, *Statistical thermodynamics for chemists and biochemists*, Springer, 1992.
75 B. M. Baynes and B. L. Trout, *J. Phys. Chem. B*, 2003, **107**, 14058–14067.
76 V. Pierce, M. Kang, M. Aburi, S. Weerasinghe and P. E. Smith, *Cell Biochem. Biophys.*, 2008, **50**, 1–22.
77 J. Smiatek, A. Wohlfarth and C. Holm, *New J. Phys.*, 2014, **16**, 25001.
78 P. E. Smith, *Biophys. J.*, 2006, **91**, 849–856.
79 P. E. Smith, *J. Phys. Chem. B*, 1999, **103**, 525–534.
80 S. Weerasinghe and P. E. Smith, *J. Phys. Chem. B*, 2003, **107**, 3891–3898.
81 E. Courtenay, M. Capp, C. Anderson and M. Record, *Biochemistry*, 2000, **39**, 4455–4471.
82 C. Wang, W. Shi, W. Zhang, X. Zhang, Y. Katsumoto and Y. Ozaki, *Nano Lett.*, 2002, **2**, 1169–1172.
83 H. Schild and D. Tirrell, *J. Phys. Chem.*, 1990, **94**, 4352–4356.
84 I. Bischofberger, D. C. E. Calzolari, P. De Los Rios, I. Jelezarov and V. Trappe, *Sci. Rep.*, 2014, **4**, 4377.
85 H. G. Schild, M. Muthukumar and D. A. Tirrell, *Macromolecules*, 1991, **24**, 948–952.
86 Y. Ono and T. Shikata, *J. Am. Chem. Soc.*, 2006, **128**, 10030–10031.
87 M. Shibayama, M. Shibayama, S.-Y. Mizutani, S.-Y. Mizutani, S. Nomura and S. Nomura, *Macromolecules*, 1996, **29**, 2019–2024.
88 Y. Lu, X. Ye, K. Zhou and W. Shi, *J. Phys. Chem. B*, 2013, **117**, 7481–7488.
89 S. Micciulla, P. A. Sánchez, J. Smiatek, B. Qiao, M. Sega, A. Laschewsky, C. Holm and R. von Klitzing, *Soft Mater.*, 2014, **12**, S14–S21.
90 A. Luzar and D. Chandler, *Nature*, 1996, **379**, 55–57.
91 D. van der Spoel, P. J. van Maaren, P. Larsson and N. Timneanu, *J. Phys. Chem. B*, 2006, **110**, 4393–4398.
92 A. Soper, E. Castner and A. Luzar, *Biophys. Chem.*, 2003, **105**, 649–666.
93 K. B. Rembert, J. Paterová, J. Heyda, C. Hilty, P. Jungwirth and P. S. Cremer, *J. Am. Chem. Soc.*, 2012, **134**, 10039–10046.
94 P. Jungwirth and P. S. Cremer, *Nat. Chem.*, 2014, **6**, 261–263.